X-ray photoelectron spectroscopy and x-ray absorption near edge structure study of copper sites hosted at the internal surface of ZSM-5 zeolite: A comparison with quantitative and...

ARTICLE *in* THE JOURNAL OF CHEMICAL PHYSICS · NOVEMBER 2000

Impact Factor: 2.95 · DOI: 10.1063/1.1319318

X-ray photoelectron spectroscopy and x-ray absorption near edge structure study of copper sites hosted at the internal surface of ZSM-5 zeolite: A comparison with quantitative and energetic data on the CO and NH_3 adsorption

V. Bolis and S. Maggiorini
DiSCAFF, Università del Piemonte Orientale ''A. Avogadro,'' v.le Ferrucci 33, 28100 Novara, Italy

L. Meda
EniChem Centro Ricerche Novara, ''Istituto G. Donegani,'' via G. Fauser 4, 28100 Novara, Italy

F. D'Acapito
INFM-OGG, c/o ESRF, GILDA CRG, BP220 F-38043 Grenoble, France

G. Turnes Palomino[a] and S. Bordiga
Dipartimento di Chimica IFM, Università di Torino, via P. Giuria 7, 10125 Torino, Italy

C. Lamberti[b]
Dipartimento di Chimica IFM, Università di Torino, via P. Giuria 7, 10125 Torino, Italy and Unità INFM Torino-Università, Torino, Italy

(Received 9 May 2000; accepted 28 August 2000)

The oxidation state of Cu species dispersed in a Cu-ZSM-5 zeolite obtained by a nonconventional gas-phase CuCl exchange, and nominally containing only Cu(I) species, was studied by x-ray photoelectron spectroscopy (XPS) and x-ray absorption near edge structure (XANES) analyses. The oxidation of Cu(I) species to Cu(II) by simple exposure to the atmosphere and subsequent reduction by thermal activation *in vacuo* was monitored. The quantitative and energetic aspects of the formation of carbonyl-like and amino-complexes at the metallic sites was studied by means of adsorption microcalorimetry. CO and NH_3 were used as probe molecules in order to assess the coordinative unsaturation of the Cu(I) cations. Adsorption heats comprised in the 130–40 kJ mol^{-1} interval were obtained for the formation of both type of complexes. The perturbation induced on the Cu centers and/or on the zeolite matrix by the adsorption of the probe molecules was monitored by parallel experiments of XPS, IR, and XANES. A significant fraction of CO and NH_3 molecules are irreversibly held on Cu(I) sites even after outgassing at room temperature (RT) at a final dynamic vacuum of 10^{-5} Torr. On the contrary, no evidence of Cu(I)/CO or of Cu(I)/NH_3 complexes was observed by XPS, indicating that such adducts are totally destroyed upon outgassing at 10^{-9} Torr. This fact implies a reconsideration of what was previously considered as a ''stable adduct.'' XPS allowed to reveal the existence of ammonia adsorbed on defective Al(III) species, and to explain the chemical nature of species formed at the earliest stages of NH_3 dosage and characterized by a heat of adsorption as high as 180 kJ mol^{-1}. By comparing the quantitative XPS and volumetric-calorimetric data it was inferred that a significant gradient of defects amount is present in the system. Finally, from the whole set of XPS measurements here reported and from parallel blank experiments on the ZSM-5 zeolite before Cu-exchange, a calibration scale for the N($1s$) peak of various nitrogen species in the different zeolite samples is proposed. © *2000 American Institute of Physics.* [S0021-9606(00)70244-3]

I. INTRODUCTION

Zeolites[1–3] are nanoporous crystalline alumosilicates constituted by corner-sharing $[TO_4]$ tetrahedra, where T represents a silicon or an aluminum atom, which chemical composition can be described by the general formula: $X^{n+}_{x/n}[(AlO_2)_x(SiO_2)_y]^{x-}$. The introduction of a trivalent Al(III) atom in a $[TO_4]$ unit [substituting the tetravalent Si(IV) atom], induces a net negative charge to zeolitic framework $(x-)$, which must be compensated by the presence of charge balancing extra-framework cations $(X^{n+}_{x/n})$. Such cations act as Lewis acid centers, being electron acceptors, but when X^{n+} are protons (H^+), the zeolite becomes a Brønsted solid acid (i.e., a proton donor). Starting from the basic $[TO_4]$ constituents, the framework of any zeolite will be realized by progressively connecting two adjacent $[TO_4]$ units by sharing an oxygen atom, which becomes so ''bridged'' between two T atoms (T–O–T).

The remarkably great flexibility of the T–O–T angle (from ≈100° up to 180°) allows us to realize, using the

[a]On leave from Departamento de Química, Universidad de las Isles Baleares, 07071 Palma de Mallorca, Spain.
[b]Author to whom correspondence should be addressed. Tel: +39011-6707841; Fax: +39011-6707858; electronic mail: Lamberti@ch.unito.it

$[TO_4]$ unit as the sole building block, an impressive large number of different zeolites,[1–3] characterized by internal voids, channels and/or cavities, of well defined size in the nanometer range (4–13 Å) accessible through apertures of well defined molecular dimensions. For these reasons, zeolites can be considered a family of solids defining a new generation of surface sites. In fact, beside the usual sites located on the top of the surface of the crystallites (external or classical surface sites), we are dealing with sites located on the surfaces defining the internal voids (internal surface sites). It is also evident that, due to their much greater relative number, the latter are those dominating the adsorptive capability of the material, at least as far as we are dealing with small molecules able to penetrate inside the internal voids. Moreover, since zeolites are easily prepared in different cationic forms,[4] cation exchange provides a means to select the nature of extraframework cations hosted at the internal surfaces of zeolites and to tune acidic strength of the Lewis intrazeolitic centers.

Metal cations grafted on the silica or alumina surface have shown a great reactivity[5–8] and the same holds for metal cations at the internal surface sites of zeolites, with the additional advantages of a much higher site density per unit volume and of the shape selectivity induced by the dimension of the cavities.

Among all copper based systems, Cu-exchanged zeolites are the most active catalysts in the selective reduction of NO_x,[9–11] showing performances much higher than those obtained on systems prepared by dispersion of Cu cations at the surface of oxides. In this particular case, the catalytic centers located at the internal surfaces of zeolites have shown to be more efficient than those located on classical surface sites. Among all Cu-exchanged zeolites, the highest yields are obtained when the metal is hosted at the internal surface of the ZSM-5 zeolite.[12]

It is generally accepted that Cu-ZSM-5 materials prepared via the so-called excess ion exchange procedure [using aqueous solutions of Cu(II) salts] are the most efficient catalysts for NO_x decomposition. For this reason, most data reported refer to highly copper-exchanged samples, normally with an exchange level higher than 100%.[13] Note that a 100% exchange is conventionally defined to occur when one Cu(II) cation substitutes two monovalent original cations (normally Na^+), resulting in a Cu/Al ratio of 0.5. In such conditions, the coexistence of copper species in different aggregation and oxidation states cannot be avoided.[14–18] From these considerations, it is evident that a structural model for Cu ions cannot consequently be confidently assessed. This is probably the reason why, in spite of the large amount of work published in recent years on these systems, the exact nature of Cu sites in ZSM-5 zeolite and their role in the catalytic processes is still on debate. This makes the elucidation of structural and catalytic properties of isolated and clustered species, which is of paramount importance in the design of an efficient catalyst, a difficult subject.

This fact has strongly suggested that the synthesis and the characterization of a pure copper-ZSM-5 model solid, containing only one oxidation state of isolated copper, could give a great help in the understanding of the structure of copper ions in zeolites and their role as catalytic centers. To achieve this goal, a nonconventional exchange route was thus followed by some of us, with the aim of directly introducing Cu(I). A pure Cu(I)-ZSM-5 sample was quantitatively prepared by directly introducing Cu(I) ions through a gas-phase reaction of H-ZSM-5 with CuCl at 573 K.[19,20] It is worth noticing that this exchange method has the further advantage to theoretically allow a 200% exchange, since when one Cu(I) cation substitute one H^+, the resulting Cu/Al ratio is 1.0. The Cu(I) environment in Cu(I)-ZSM-5 samples so prepared was already studied by EXAFS, IR, EPR, and UV-VIS spectroscopies as reported in Ref. 21.

In the present work we report a combined x-ray photoelectron spectroscopy (XPS), x-ray absorption near edge structure (XANES), and microcalorimetric study aimed at three different goals: (i) To further prove that the oxidation state of Cu sites present at the internal surface of the as-prepared sample is +1; (ii) to determine the redox capability of the surface Cu(I) ions upon exposure to air and subsequent thermal activation; and (iii) to investigate the formation of surface adducts of CO and NH_3 in an extremely large equilibrium pressure range (10^2–10^{-9} Torr: 1 Torr≈133 kPa).

II. EXPERIMENT

Cu(I)-ZSM-5 was prepared starting from a NH_4-ZSM-5 sample (Si/Al=14, EniChem SpA, Centro Ricerche di Novara) by using a nonconventional gas-phase exchange employing CuCl. The exchange procedure was done in two steps. A thermal treatment *in vacuo* (dynamical) of 10^{-3} Torr at 673 K allowed the ammonium ions to be decomposed yielding the protonic form of the zeolite and ammonia gas,

$$\mathrm{Si{-}(ONH_4)^+{-}Al^-} \rightarrow \mathrm{Si{-}(OH)^+{-}Al^-} + \mathrm{NH_3}. \quad (1)$$

The subsequent interaction with gaseous CuCl, sublimated *in situ* by opening the connection with an adjacent section of the preparation cell, gives rise to the desired cuprous form of the zeolite and to hydrogen chloride gas,

$$\mathrm{Si{-}(OH)^+{-}Al^-} + \mathrm{CuCl} \rightarrow \mathrm{Si{-}(OCu)^+{-}Al^-} + \mathrm{HCl}. \quad (2)$$

More details on the exchange procedure are reported elsewhere.[20] It is worth noticing that, in order to achieve the highest copper loading, an excess CuCl is dosed; as a consequence, upon cooling down the temperature of the sample, clusters of unreacted CuCl are trapped inside the zeolite channels. Excess CuCl is then eliminated easily by heating the zeolite powder at 673 K in order to allow CuCl to sublimate (*vide infra* Sec. III A). A nearly total exchange was obtained [corresponding to one Cu(I) cation for every framework Al atom] as evidenced by the virtually total absence of the O–H stretching band of bridged Si–(OH)–Al groups (spectra similar to those reported in Fig. 1 of Ref. 21 and thus not reported for the sake of brevity).

XPS measurements were performed by means of a PHI-5500 spectrometer with a monochromatized Al-$K\alpha$ source. Samples in slices were prepared by pressing catalyst powder to produce flat surfaces. An electron gun was used to neutralize surface charging occurring for insulating samples. The peak of C(1*s*) at 285.0 eV, due to carbonaceous residual of the template burning, was used as internal calibration of the

energy scale. The analysis was performed at a power as low as 100 W in order to minimize possible reduction of copper species induced by irradiation. Adsorption–desorption cycles of CO and NH_3 were performed at RT in a specially designed prechamber. The sample was outgassed at 673 K (2 h, 10^{-9} Torr) prior to the first adsorption measurements. The maximum equilibrium pressure reached in any case was ≈10 Torr. Before any XPS analysis the sample was transferred into the analysis chamber without exposure to the atmosphere, and there outgassed at RT until a final vacuum of 10^{-9} Torr.

The heats of adsorption (q_{ads}) were measured at 303 K by means of a heat-flow microcalorimeter (Tian-Calvet-type, Setaram-France) in order to evaluate the enthalpy changes related to the adsorption process ($q_{ads} = -\Delta_{ads}H$). A well-established stepwise procedure, previously described,[22] was followed. The calorimeter was connected to a high vacuum ($p \leqslant 10^{-5}$ Torr) gas-volumetric glass apparatus, that enabled to determine simultaneously the adsorbed amounts (Δn_{ads}) and the heats evolved (ΔQ^{int}) for small increments of the adsorptive.

Thanks to the differential construction of the apparatus, all parasite effects other than the one due to the interaction of the gas with the surface of the solid studied could be compensated. The adsorbed amounts ($n_{ads} = \Sigma \Delta n_{ads}$) and the heat evolved ($Q^{int} = \Sigma \Delta Q^{int}$) were so determined at increasing equilibrium pressure of the adsorptive. The amounts adsorbed per gram of zeolite are reported as a function of the equilibrium pressure (volumetric isotherms, n_{ads} vs p), whereas the calorimetric isotherms (Q^{int} vs p) will not be reported for the sake of brevity. The integral heats (Q^{int}) evolved during the adsorption process are reported as a function of the increasing adsorbed amounts (n_{ads}). The differential heat of adsorption (q^{diff}) is defined as the derivative of the $Q^{int} = f(n_{ads})$ curves; a polynomial of the form $Q^{int} = \Sigma a_k n_{ads}^k$ was used to fit by least squares the integral heat curves. Alternatively, the differential heat values can be obtained by drawing a continuous curve passing through the middle points of the experimental histogram of the partial molar heats ($\Delta Q^{int}/\Delta n_{ads}$, kJ/mol) (Ref. 23) for incremental doses of the adsorptive as a function of the adsorbed amounts n_{ads}. Whatever method was employed, the differential heats of adsorption are here reported as a function of the coverage (q_{ads} vs n_{ads}). The initial heat value (q_0), corresponding to the highest energy of interaction of the probe with the strongest sites, was evaluated by extrapolating to zero coverage the heat vs coverage plots.

The detection threshold of the microcalorimeter is 50 μJ per impulsion. In all cases considered in the present work the heat evolved during the adsorption of each single dose of the adsorptive ranged between 0.10 and 1.0 J. A first run of adsorption was performed on the samples previously outgassed at 673 K (2 h, 10^{-5} Torr). The second and third runs were performed after outgassing the sample at the calorimeter temperature either overnight (14 h) or during the weekend (60 h), at 10^{-5} Torr, in order to evaluate the contribution of the reversible (in the adopted conditions) component to the adsorption. The equilibrium pressure was monitored by means of a transducer gauge (Barocel 0–100 Torr, Edwards).

XANES experiments were performed at the GILDA MB8 beamline[24] at the European Synchrotron Radiation Facility (ESRF) during experiment CH-542.[25] The monochromator was equipped with two Si(311) crystals while harmonic rejection was achieved using mirrors. In order to assure very high quality XANES spectra, the geometry of the beamline was optimized to improve the energy resolution; vertical slits, located at 23 m from the source, were set to 0.6 mm assuring, at 9 keV, an actual energy resolution better than 0.5 eV. XANES spectra were collected with a sampling step of 0.2 eV and an integration time of 3 s/point. The following experimental geometry was adopted: (i) I_0 (800 Torr N_2 filled ionization detector having efficiency of 10%); (ii) zeolite sample; (iii) I_1 (80 Torr Ar filled ionization detector having efficiency of 50%); (iv) 7 μm thick copper metal foil; (v) I_2 (photodetector). This set-up allows a direct energy/angle calibration for each spectrum avoiding any problem related to little energy shifts due to small thermal instability of the monochromator crystals. This experimental geometry implies that the dynamical focusing mode, available at the GILDA BM8 beamline,[24] was not used. The first maximum of the XANES derivative spectrum of the Cu metal foil, corresponding to the $1s \rightarrow 4p$ electronic transition of Cu(0), was defined as 8979.0 eV.

For IR measurements, a thin self-supporting wafer of the zeolite was prepared and activated under a dynamical vacuum ($p \approx 10^{-4}$ Torr) at 673 K for 2 h, inside an IR cell designed to allow *in situ* both high temperature treatments and gas dosage, and low-temperature measurements. The IR spectra were recorded at 2 cm^{-1} resolution on a BRUKER FTIR 66 spectrometer equipped with an HgCdTe cryodetector.

III. RESULTS AND DISCUSSION

A. On the oxidation state of copper: An XPS and XANES study

The instability of surface cuprous ions upon the combined action of O_2 and H_2O, present in the atmosphere, makes the handling and the measurements of Cu(I) containing samples very delicate. In the present case, the excess CuCl formed in the adopted preparation procedure (*vide supra* Sec. II) occludes the zeolite channels preventing the oxidation of the internal Cu(I) surface sites. The excess of unreacted CuCl plays thus the role of a protective cap and allows to handle the exchanged sample without special cautions. The pure Cu(I)-ZSM-5 will be so obtained by heating under dynamical vacuum the sample *in situ* before the experiment (XPS, XANES, IR, and microcalorimetry) at a temperature sufficiently high to allow CuCl sublimation.

XPS is a widely used technique to investigate the oxidation states of surface species. According to standard binding energy (BE) values,[26] Cu(I) species exhibit the $2p(3/2)$ peak in the 932.2–932.8 eV region (Cu_2S, CuCl, and Cu_2O), while for Cu(II) species the peak is shifted to higher energies such as 933.7 eV for CuO or as 935.0 eV for $CuCl_2$. A similar behavior is observed for the parent $2p(1/2)$ peak. Moreover, Cu(II) species exhibit two additional broader shake-off bands in the 941–946 eV and 961–965 eV regions.

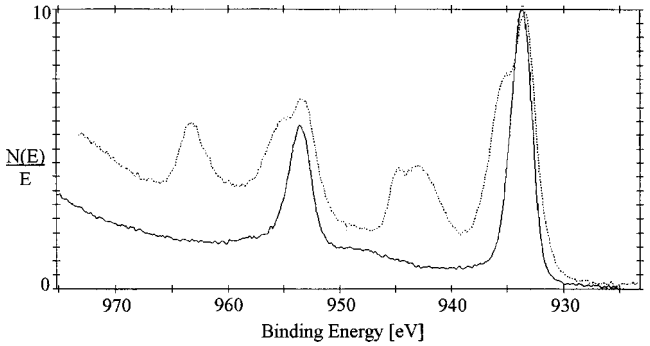

FIG. 1. XPS spectra, in the Cu($2p$) spectral range, of the Cu-ZSM-5 sample before (dotted line) and after (full line) removal of the excess CuCl.

Unfortunately, the $2p(3/2)$ and $2p(1/2)$ peaks of Cu(0) are virtually indistinguishable from those of Cu(I).

For these reasons XPS was used to study copper zeolites by several groups.[17,27–34] In this work, we have used XPS to verify whether the CuCl protective cap is really able to prevent the oxidation of the internal Cu(I) sites. Figure 1 reports, in the Cu($2p$) spectral range, the XPS spectra of the Cu(I)-ZSM-5 before and after removal of the excess CuCl. The first spectrum (dotted line) clearly indicates that, at the surface of the as-exchanged sample, copper atoms are present in both (I) and (II) oxidation states. This reflects the fact that the external surface of the CuCl cap has been partially oxidized by air to $CuCl_2$. Upon *in situ* sublimation of copper chlorides, by heating the sample in the prechamber up to 673 K, an XPS spectrum where Cu(II) species are virtually absent was obtained (see full line curve in Fig. 1). This datum means that no Cu(II) species are virtually present at the internal surface of the zeolite. By looking to the Cu $L_3M_{45}M_{45}$ transitions (not reported for brevity), no evidence of Cu(0) species was found. However, owing to the fact that Cu(0) species are hardly distinguished from Cu(I) ones, the presence of a small fraction of the former species cannot be safely ruled out on the basis of XPS data only.

For this reason XANES measurements were performed. In fact, because of the great differences among the pre-edge spectra of Cu(0), Cu(I), and Cu(II) species, XANES spectroscopy has often been used to distinguish the different oxidation state of copper species in zeolites.[13–15,17,21,35–41] In fact, the most evident pre-edge feature in the XANES spectra of copper is the dipole-allowed $1s\rightarrow 4p$ electronic transition, which occurs at progressively higher energies by increasing the oxidation state of Cu. This pre-edge peak is observed in the 8977–8980 eV, 8983–8984 eV, and 8985–8988 eV regions for Cu(0), Cu(I), and Cu(II) species, respectively. This is clearly visible in the XANES spectra of Cu metal, CuCl and $CuCl_2$ model compounds reported in Fig. 2 (top spectra). In spite of what was observed by XPS, the XANES spectrum of sample measured before CuCl elimination (fourth from top in Fig. 2) has the typical feature of copper in the oxidation state +1. This implies that the oxidation to cupric species occurs only at the external surface and does not penetrate inside the channels, resulting in a nonsignificant contribution to the overall XANES signal. From the XANES spectra reported in Fig. 2 (before and after CuCl elimination)

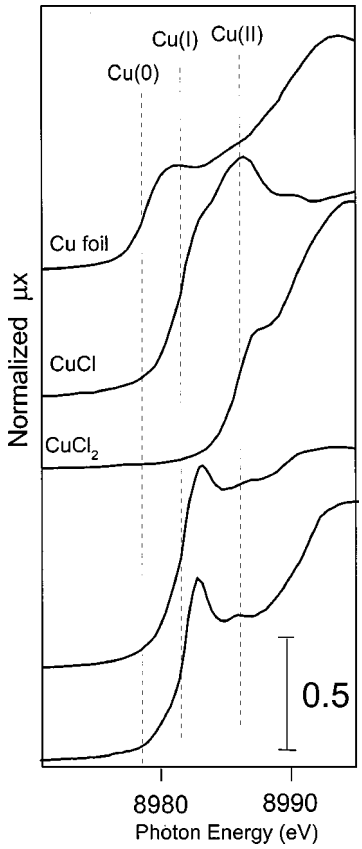

FIG. 2. XANES spectra of, from top to bottom: Cu metal foil, CuCl, $CuCl_2$, and Cu-ZSM-5 sample before and after removal of the excess CuCl. Vertical dotted lines reports the position (maximum of the first derivative) of the dipole-allowed $1s\rightarrow 4p$ electronic transition, for Cu(0), Cu(I), and Cu(II) species.

the presence of a fraction of clustered Cu(0) species can be safely ruled out, since no significant absorption is observed in the 8977–8980 eV region. On the contrary, the small fraction of Cu(II) species could not be detected, since a small absorption in the 8985–8988 eV region would be totally overshadowed by the $1s\rightarrow 4p$ peak occurring a few eV below and successive photoelectric edge of the Cu(I) species which are predominant in such samples.

The relevance of the combined use of XPS and XANES in the evaluation of the valence state of copper impurities in a Cu(I) sample stems on the fact that the former is able to reveal even very small fractions of Cu(II) species, while the latter is able to easily determine even traces of Cu(0) species. We can so conclude this preliminary study by confirming that the so prepared zeolite contains, within the sensitivity of the adopted techniques, only cuprous counterions. This is in agreement with a previous study,[21] where we estimated, by a combined IR and EPR study, that the fraction of Cu(I) was 99% of the total copper.

The virtually total elimination of unreacted copper chlorides was evidenced on the basis of XPS elemental analysis too. In fact, the Cu/Al ratio falls, upon sample activation, from 2.6 to 1.1, a value very close to the expected 1.0 ratio and the chlorine at % falls from 4 down to the detection threshold. In all XPS spectra (before and after activation, CO and NH_3 dosage) we found a rather good reproducibility of

the Si/Al ratio, which lies always in the 10–13 range. This can be considered as a good result, since the experimental error in the determination of the Si/Al ratio is mainly affected in the error associated with the determination of the aluminum at %, since Al is a rather diluted species in the sample (in the order of 2 at %). Finally, it is worth noticing that a carbon and a nitrogen contamination was observed. The presence of both C and N atoms is not unexpected, since due to the carbonaceous and aminic residual formed inside the zeolite channels upon template (tetra-propylammonium ions) burning.[27,31]

B. On the redox cycle of copper: An XPS and XANES study

The study of the Cu(I)↔Cu(II) redox properties of this material is of fundamental relevance, since a Cu(I)↔Cu(II) redox cycle is the key mechanism in the catalytic decomposition of nitric oxides promoted by Cu-ZSM-5, see, e.g., Refs. 20, 21, and 42.

For this reason the ability of Cu(I) sites to undergo a complete oxido–reductive cycle was studied. The oxidation step of the cycle was performed by exposing the activated sample to air for one day, while the subsequent reduction step was performed in successive thermal treatments. It is in fact widely recognized[27,31,37,43–48] that an effective reduction of samples containing hydrated cupric ions can be obtained by heating the Cu(II) containing samples under dynamical vacuum. This fact is often called ''self-reduction'' of Cu(II). Different chemical Cu(II)→Cu(I) pathways have been proposed in the literature to explain the process. We will not enter in this complex debate here and we shall just accept the phenomenon as a matter of fact. For a more detailed discussion, the reader should refer to the recent works of Dossi *et al.*[30] and of Turnes Palomino *et al.*[37]

As far as the oxidation step is concerned, exposure to air of the sample for one day at RT led to a nearly total oxidation of Cu(I) sites to Cu(II). This is clearly visible from both XPS and XANES spectroscopies, see Figs. 3(a) and 4 (top curve), respectively, where spectral features typical of Cu(II) species are clearly evident.

Coming to the thermal reduction process, we performed it in a progressive way in order to follow the phenomenon step by step. As far as XPS measurements are concerned, two different procedures were adopted: (i) successive thermal treatments under vacuum conditions at increasing temperatures 293, 373, 473, 573, and 673 K and (ii) successive treatments under vacuum conditions at 723 K for increasing times 2, 4, and 6 h. Due to the limited beam-time available at the synchrotron, only procedure (i) has been followed for XANES experiments. Figure 3 reports the XPS spectra collected following procedure (ii). A similar trend was observed following procedure (i), spectra not reported for brevity. From Fig. 3, the successive Cu(II)→Cu(I) reduction is evident. The same holds for the XANES spectra reporting the reduction obtained with procedure (i), see Fig. 4.

The relative amounts of Cu(I) and Cu(II) species were estimated on the basis of a band fitting procedure performed on the Cu($2p3/2$) XPS signal using two Gaussian curves centered at 933.4 and 935.4 eV for Cu(I) and Cu(II) species,

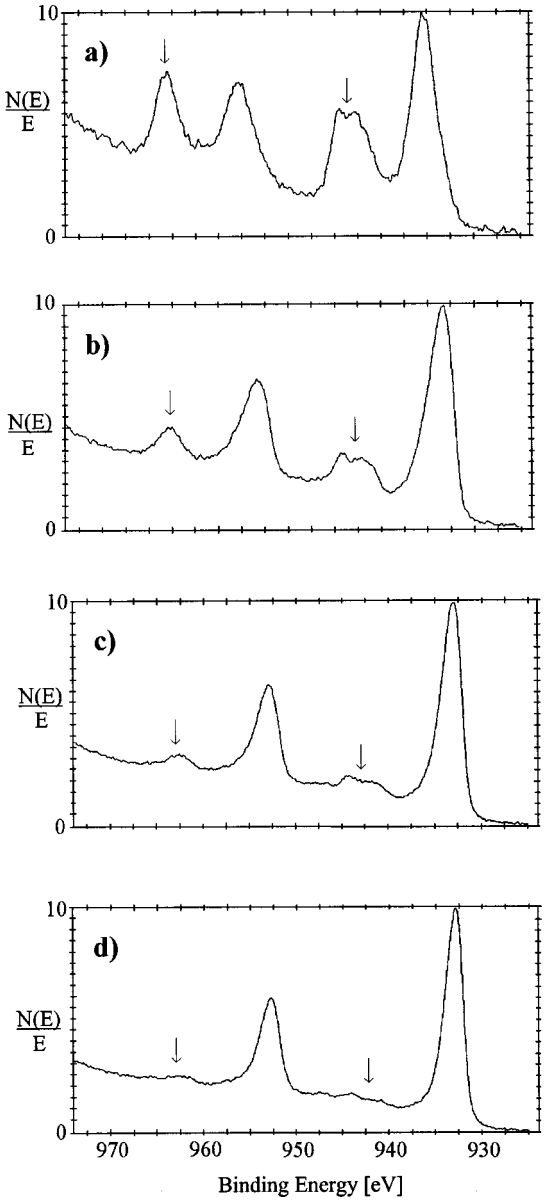

FIG. 3. XPS spectra, in the Cu($2p$) spectral range, of the activated Cu-ZSM-5 sample exposed to air for one day (a), and after thermal reactivation at 723 K for 2, 4, and 6 h, parts (b), (c), and (d), respectively.

respectively, see Table I. After exposure to air for one day, (oxidized sample) the band fitting indicates a Cu(II) fraction of 0.95; however, a band fitting using a unique Gaussian curve centered at 935.4 eV was able to fit the experimental curve rather well. We can thus conclude, within the sensitivity limits of the technique, that exposure to air for one day led to a virtually total oxidation of copper sites. Thermal activation at 723 K for 2, 4, and 6 h lead to a progressive restoration of the original Cu(I) species (estimated fraction of 0.6, 0.7, and 0.8, respectively). The same holds for the reduction procedure (i) followed by both XPS (not reported) and XANES (Fig. 4).[49]

A final point deserves a comment. The bottom spectrum of Fig. 4, i.e., the XANES spectrum of the sample virtually containing only Cu(I) species clearly presents a second peak 2.9 eV above the most intense one. This is due to a perturbation effect on the threefold degenerated $4p_{x,y,z}$ orbital of a

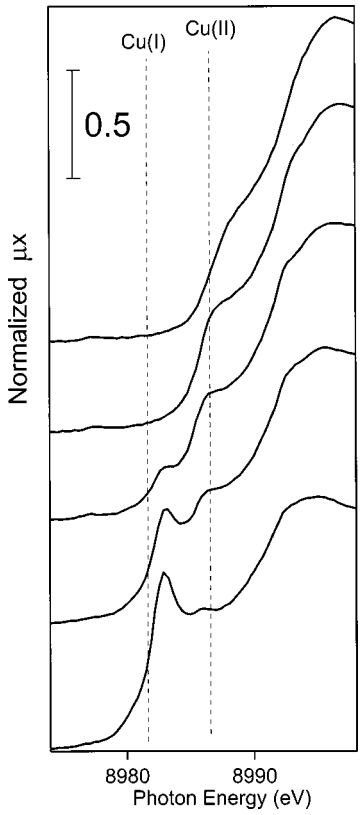

FIG. 4. XANES spectra of activated Cu-ZSM-5 sample, from top to bottom: exposed to air for one day, and after thermal reactivation for 2 h at 373, 473, 573, and 673 K. Vertical dotted lines as in Fig. 2, for Cu(I) and Cu(II) species.

free Cu(I) ion, which is split by the ligand field into $4p_{x,y}$ and $4p_z$ levels.[50,51]

We can so conclude this XPS and XANES study by stating that all original Cu(I) sites are virtually oxidized to Cu(II) upon exposure to air, and that a small fraction of Cu(II) resists to the thermal reduction under the adopted conditions. We feel that a virtually total reduction could be reached if more severe thermal conditions (either by increasing the temperature or by increasing the activation time) would be applied. This means that virtually all copper sites are surface sites and thus easily reached by the oxidation agents of the atmosphere and subsequently re-reduced to Cu(I) by thermal treatments. This, in turn, suggests that all copper sites of this sample are potentially active in the catalytic decomposition of NO_x.

C. On the interaction with probe molecules: An XPS, IR, microcalorimetric and XANES study

The high activity of Cu(I)-ZSM-5 zeolite, as compared to other supported copper catalysts, is probably related to the high coordinative unsaturation of extra-framework Cu(I) ions hosted in the MFI matrix.[21,52] These ions are known to have a high reactivity, as demonstrated by the formation of different end-on adducts stable at RT at an equilibrium pressure of some 80 Torr: $[Cu(N_2)]^+$ (Refs. 21 and 53), $[Cu(CO)]^+$ and $[Cu(CO)_2]^+$ (Refs. 19 and 21), and $[Cu(NH_3)_4]^+$ (Ref. 54). By lowering the pressure down to 10^{-4} Torr we observe that: (i) $[Cu(N_2)]^+$ species are totally destroyed;[21,53] all $[Cu(CO)_2]^+$ complexes lose one CO ligand but at about 50% of the sites the $[Cu(CO)]^+$ complexes are firmly held at the surface;[19,21] (iii) about 50% of $[Cu(NH_3)_4]^+$ complexes lost two ammonia ligands, while the remaining species lose three of them, giving rise to stable $[Cu(NH_3)_2]^+$ and $[Cu(NH_3)]^+$ species. From this brief overview, it is evident that not all the complexes stable at an equilibrium pressure of the gas of 80 Torr are observed by decreasing the pressure of about five orders of magnitude. The $10^{-4}/10^{-5}$ Torr range is a lower limit for the pressure in experiments carried out by using conventional IR, XANES or microcalorimetric apparatuses.

In this regard, it is evident that XPS, being intrinsically an ultrahigh vacuum technique, offers the possibility to investigate a complete different passage range domain, gaining five further order of magnitudes and reaching pressure limits as low as 10^{-9} Torr. For this purpose, N_2 probe was not suitable, since totally desorbed by outgassing at only 10^{-4} Torr.[21,53] In order to investigate the whole range of equilibrium pressures from 10^2 to 10^{-9} Torr CO and NH_3 were chosen as probes, owing to their rather strong affinity for Cu(I) sites.

1. CO adsorption

a. IR spectroscopy of adsorbed CO: IR spectroscopy of adsorbed CO at RT on Cu(I)-ZSM-5 is very informative. At low equilibrium pressure a single and well defined band at 2157 cm^{-1} indicates the formation of mono-carbonyl $[Cu(CO)]^+$ species. By increasing the equilibrium pressure, the band grows up to a maximum value and then progressively decreases with the parallel formation of two new bands at 2178 and 2151 cm^{-1} witnessing the formation of di-carbonyl $[Cu(CO)_2]^+$ species. These bands are assigned to the symmetric and asymmetric stretching frequencies of the di-carbonyl species.[20,21,36,55] The progressive evolution of

TABLE I. Deconvolution of the Cu($2p3/2$) signal with two Gaussian curves centered at 933.4 and 935.4 eV and subsequent evaluation of the Cu(I) and Cu(II) fractions for the Cu-ZSM-5 sample activated and exposed to air and for subsequent thermal treatments at 723 K for increasing times.

Activation time at 723 K	XPS Cu(II) ($2p3/2$) peak Intensity (a.u.)	FWHM (eV)	XPS Cu(I) ($p3/2$) peak Intensity (a.u.)	FWHM (eV)	$\frac{Cu(II)}{[Cu(II)+Cu(I)]}$	%Cu(II)	%Cu(I)
···	8207±90	3.3±0.1	432±20	1.9±0.1	0.950	95±10	5±10
2 h	4089±65	3.3±0.1	6202±80	2.4±0.1	0.397	40±10	60±10
4 h	3854±60	3.2±0.1	10 031±100	2.3±0.1	0.278	30±10	70±10
6 h	2561±50	3.0±0.1	12 448±110	2.1±0.1	0.171	20±10	80±10

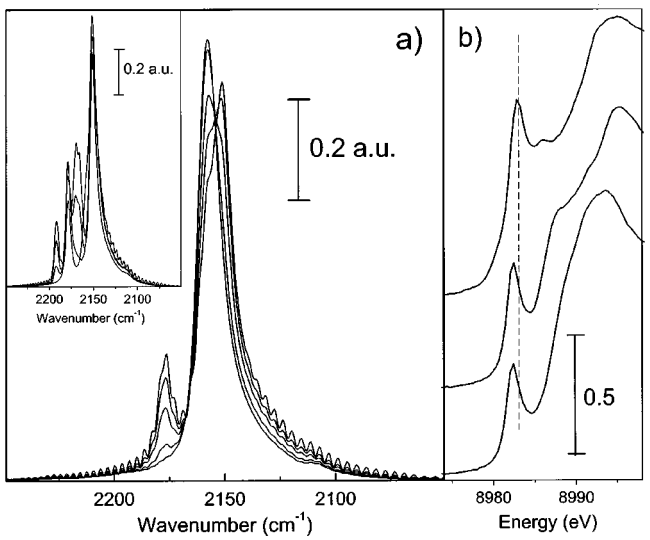

FIG. 5. (a) IR spectra, in the C–O stretching region, of CO molecules dosed (at RT) at increasing equilibrium pressures (10^{-3}–40 Torr) on the activated Cu(I)-ZSM-5 sample. The spectrum collected before CO dosage was used as background: all reported spectra are background subtracted. The inset reports the same experiment performed at liquid nitrogen temperature. (b) XANES spectra of, from top to bottom: Cu(I)-ZSM-5 sample *in vacuo*, after interaction with 1 and 40 Torr of CO. The formation of copper mono- and di-carbonylic complexes causes a remarkable modification of XANES spectra owing to a significant variation in both electronic configuration and local environment of the Cu(I) species. Vertical dotted line marks the position of the $1s \rightarrow 4p$ peak for the first spectrum.

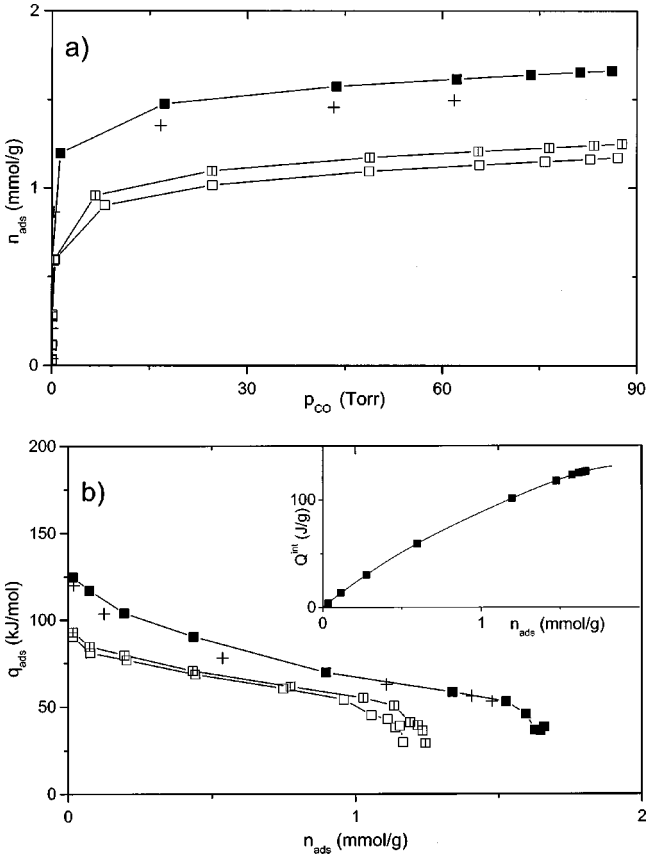

FIG. 6. (a) Volumetric isotherms of CO adsorbed at 303 K on Cu-ZSM-5 activated at 673 K (solid symbol: 1st run; open symbols: 2nd run; barred symbols: 3rd run) and on Cu-ZSM-5 exposed to air and reduced *in vacuo* at 673 K (cross symbols, 1st run). (b) Differential heat of adsorption of CO on the samples described in part (a), as a function of the adsorbed amounts. Symbols as in part (a). Inset: integral heats of adsorption as a function of the adsorbed amounts. The interpolated line has been obtained by a polynomial regression, $Q^{int}=a+b_1 n_{ads}+b_2 n_{ads}^2+b_3 n_{ads}^3+b_4 n_{ads}^4+b_5 n_{ads}^5$ ($a=0.35$; $b_1=117.79$; $b_2=-25.53$; $b_3=-24.52$; $b_4=28.70$; $b_5=-8.34$).

the spectral features is clearly visible in Fig. 5(a), where the presence of two isosbestic points at 2167 and 2154 cm^{-1} clearly demonstrates that the growth of the 2178 and 2151 cm^{-1} bands occurs to the detriment of the 2157 cm^{-1}. This experimental evidence implies that the formation of $[Cu(CO)_2]^+$ adducts occurs only when all Cu(I) sites have been saturated by forming mono-carbonyl $[Cu(CO)]^+$ adducts. This will be of great help in the assignment of the adsorption heats values for the formation of the different complexes (*vide infra* microcalorimetric data). Prolonged outgassing at RT (10^{-4} Torr) causes the total disruption of the di-carbonyl adducts and a reduction to about 50% of the 2157 cm^{-1} band with respect to its maximum value. This clearly means that a significant fraction of the $[Cu(CO)]^+$ adducts formed inside the zeolite chemicals are stable upon outgassing at 10^{-4} Torr, as will be both qualitatively and quantitatively confirmed by XANES and microcalorimetric results, respectively.

It is finally worth noticing that the virtually total elimination of unreacted CuCl, already demonstrated for the external surfaces by XPS elemental analysis, was proven by IR spectroscopy of CO adsorbed at 100 K for the internal surface too. In fact, CO dosed at the liquid nitrogen temperature on CuCl gives rise to a well defined C–O stretching band at 2134 cm^{-1}.[56] This feature was not observed in the IR spectra of CO dosed at the same low temperature on the activated Cu-ZSM-5 sample, see inset in Fig. 5(a), where only the $[Cu(CO)_2]^+ \rightarrow [Cu(CO)_3]^+$ transformation is observed.[20,21]

b. XANES and XPS spectroscopy of adsorbed CO: Adsorption of CO, resulting in the formation of $[Cu(CO)]^+$ and $[Cu(CO)_2]^+$ adducts, causes a strong modification of both pre-edge and near-edge regions in the XANES spectra of Cu(I), as documented in Fig. 5(b). As far as the pre-edge region is concerned, we note a significant decrease and a progressive shift towards lower energies of the $1s \rightarrow 4p$ peak, indicating that the electronic configuration of copper is strongly affected by the formation of $[Cu(CO)]^+$ and $[Cu(CO)_2]^+$ adducts. On the basis of this evidence, we expected to see significant modifications also in the XPS spectra, as a consequence of the formation of copper carbonyl species. On the contrary, no appreciable difference neither in the XPS Cu($2p3/2$), Cu($2p1/2$), Cu($3s$), and Al($2s$) nor in the Auger Cu($L_3M_{45}M_{45}$) peaks was detected upon dosing CO on Cu(I)-ZSM-5 sample in the XPS prechamber. Moreover, no significant increase of the C($1s$) due to carbonaceous contaminants (*vide supra*) was observed. We must so conclude that $[Cu(CO)]^+$ complexes, which are stable at 10^{-4} Torr, are totally destroyed upon adopting the much more severe vacuum conditions needed to perform the XPS experiment.

c. Calorimetric data of adsorbed CO: In Fig. 6(a) the volumetric isotherms of CO adsorbed at 303 K on Cu-ZSM-5 zeolite are reported. The curves refer to the total

TABLE II. Quantitative and energetic data of the adsorption of CO and NH_3 on Cu(I)-ZSM-5 zeolite at 303 K.

p_{CO} (Torr)	n_{ads} (mmol/g)	Molecules/Cu(I) cation	q_{ads} (kJ/mol)
20	1.49[a]	1.42[a]	58[a]
20	0.98[b]	0.94[b]	56[b]
20	1.06[c]	1.01[c]	56[c]
80	1.65[a]	1.58[a]	35[a]
80	1.17[b]	1.12[b]	36[b]
80	1.23[c]	1.18[c]	36[c]
p_{NH_3} (Torr)	n_{ads} (mmol/g)	Molecules/Cu(I) cation	q_{ads} (kJ/mol)
20	3.57[a]	3.41[a]	49[a]
20	1.61[b]	1.54[b]	46[b]
20	1.82[c]	1.74[c]	46[c]
80	4.95[a]	4.73[a]	38[a]
80	3.04[b]	2.91[b]	33[b]
80	3.23[c]	3.09[c]	33[c]

[a]1st run of adsorption.
[b]2nd run of adsorption.
[c]3rd run of adsorption.

adsorption (1st run) on the sample thermally activated at 673 K and the reversible adsorption on the same sample first outgassed overnight, 14 h (2nd run) and then outgassed during the weekend, 60 h (3rd run). The cross symbols correspond to the amount of CO adsorbed on the Cu-ZSM-5 sample thermally reactivated *in vacuo* after exposure to air. In section b of the figure the correspondent differential heats of adsorption vs coverage plots are reported. The differential heats of adsorption were obtained by differentiating the Q^{int} vs n_{ads} curve reported in the inset of the figure, and were found virtually identical to the values obtained by the experimental histogram of the partial molar heats ($\Delta Q^{int}/\Delta n_{ads}$, kJ/mol) as a function of the adsorbed amounts n_{ads} (not reported for the sake of brevity). The Q^{int} vs n_{ads} curves for the 2nd and 3rd runs are not reported also for the sake of brevity and clarity.

Let us consider first the adsorption of CO on the Cu(I) sites present on the pristine activated Cu-ZSM-5. It can be noticed that the interaction of CO with coordinatively unsaturated (*cus*) Cu(I) cations involves the formation of carbonyl-like species [see IR spectra in Fig. 5(a)] that are only partially unstable upon outgassing under the conditions adopted in the experiment ($p \approx 10^{-5}$ Torr). In fact the 1st and 2nd (after outgassing overnight) runs of adsorption are not coincident. The difference between the two curves at any given equilibrium pressure corresponds to the amount of adsorbate irreversibly held at the surface, i.e., to the amount of carbonyl-like species sufficiently stable to resist outgassing at a final vacuum of 10^{-5} Torr. For instance, at an equilibrium pressure of 80 Torr the total adsorbed amounts are 1.65 mmol/g of zeolite whereas the reversible amounts are 1.15 mmol/g, indicating that only 69.7% of the carbonyl-like species formed are labile in the conditions of outgassing adopted, in contrast with what was found in the XPS experiments. By prolonging the outgassing at $p \approx 10^{-5}$ Torr for 60 h the amount of labile adducts increases but not very much; the fraction of the reversible component is now 74.5%. In Table II the quantitative and energetic data of CO adsorbed at $p_{CO}=20$ and 80 Torr are reported and compared with the analogous data obtained for NH_3 adsorption (*vide infra*).

The total amount of CO adsorbed (1st run) at the equilibrium pressure finally reached ($p_{CO} \approx 80$ Torr) corresponds to a number of CO molecules per Cu(I) cation of ≈ 1.6 (see the volumetric isotherm). This figure underestimates somehow the number of CO molecules adsorbed per Cu(I) cation, in that at the final pressure of CO reached in the experiment the adsorption isotherm has not yet reached the saturation. Thus, the number of CO molecules adsorbed per Cu(I) cation can be reasonably considered close to two, suggesting that all Cu(I) cations do form the mono-carbonyl $[Cu(CO)]^+$ adducts and that the majority of these species tend to evolve to the formation of the di-carbonyl $[Cu(CO)_2]^+$ species.[54]

The evolution of the heat of adsorption with coverage indicates that the Cu(I) sites are relatively heterogeneous with respect to the probe used, in that the differential heat of adsorption continuously decreases from an initial value of ≈ 130 kJ/mol down to ≈ 40 kJ/mol. Indeed, the slope of the Q^{int} vs n_{ads} curve (obtained by a polynomial of order 5; see the parameters in the caption of the figure) continuously decrease in the whole range of coverage examined. The number of sites interacting with an energy higher than 100 kJ/mol is quite low, and corresponds to the adsorption of ≈ 0.3 CO molecules per Cu(I) cation ($<20\%$ of the total molecules adsorbed at an equilibrium pressure of 80 Torr), giving rise to the formation of a few quite stable and energetic monocarbonyl species [see IR spectra reported in Fig. 5(a)]. The high value of the initial heat of adsorption of CO on the coordinatively unsaturated Cu(I) cations suggests that a chemical bond of carbonyl type is formed, involving both σ-coordination and π-back-donation. This suggestion is supported by the value of the ν_{CO} stretching frequency quite low with respect to the one expected on the basis of the charge/size ratio of the Cu(I) cations.[57] The heat of adsorption of the reversible component of the process is definitely lower in the all range of coverage examined and ranges in the 90–40 kJ/mol interval. It corresponds on one hand to the formation of less energetic mono-carbonyl species and on the other hand to the addition of a second CO molecule giving rise to di-carbonyl species. By comparing the 2nd and 3rd run curves, it can be noticed that the latter one lies slightly higher than the former one in the all range examined, indicating that the prolonged outgassing allows an additional fraction of CO molecules more strongly bound to be desorbed.

By considering the following dissociation equilibrium of the carbonyl adducts:

$$[Cu(CO_2)]^+_{surf} + CO_{(gas)} \Leftrightarrow [Cu(CO)]^+_{surf} + CO_{(gas)} \Leftrightarrow Cu^+_{cus} + CO_{(gas)}, \quad (3)$$

the ultrahigh-vacuum conditions (UHV) allow the equilibrium to be completely shifted to the right involving a virtually complete dissociation of the complexes. This means that the vacuum conditions chosen in the individual experiment (10^{-9} Torr for XPS ones and 10^{-4}–10^{-5} Torr for IR and adsorption microcalorimetry ones) determine the extent of the stability of the adducts formed under an equilibrium pres-

sure of CO. However, besides the fact that XPS results indicate that all carbonyl-like species are labile upon UHV outgassing, IR and calorimetric data allow to make a distinction in the stability of the adducts. In particular, from a quantitative point of view it was observed that only less than 1.5 molecules of CO per Cu(I) cation are desorbed by outgassing in relatively mild conditions ($p \approx 10^{-5}$ Torr). The IR evidence indicates that in these conditions the di-carbonyl species are completely destroyed, whereas the mono-carbonyl species only partially. From an energetic point of view it is not possible to clearly separate the contribution to the heat of adsorption due to the addition of the second CO molecule from the contribution due to the formation of the less stable mono-carbonyl species. In fact the heat of adsorption curves decrease continuously without indicating the saturation of one species and the starting up of the other. Nevertheless, we can tentatively assign the higher values of the heat of adsorption to the formation of mono-carbonyl species, thanks to the IR spectroscopy indication that the di-carbonyl species start to form when the mono-carbonyl peak does not increase anymore [see IR spectra in Fig. 5(a)].

As for the sample re-activated *in vacuo* after the oxidation caused by the exposition to air, the heat of adsorption of CO is only slightly reduced (mostly at low coverage) with respect to the pristine sample, as shown in Fig. 6(b) (see cross symbols), indicating that only a few energetic Cu(I) sites were lost during the oxidation-reduction cycle. The amount of CO adsorbed are lower of less than 10% of the total amount adsorbed on the pristine sample [see Fig. 6(a), cross symbols], confirming what was suggested by XPS data (see Table I) that a small but not negligible fraction of Cu(I) sites were not completely restored by the thermal treatment *in vacuo*, at least in the conditions adopted during the present experiments.

2. NH_3 adsorption

a. Calorimetric data of adsorbed NH_3: In Fig. 7 the volumetric isotherms (1st, 2nd, and 3rd runs) of NH_3 adsorbed on the pristine Cu-ZSM-5 sample outgassed at 673 K (section a) are reported. In sections b and c, the differential (1st, 2nd, and 3rd runs) and the integral (only the 1st run, for the sake of brevity and clarity) heats of adsorption are reported as a function of coverage. The differential heats reported in the plots of section b were obtained by the experimental histogram of the partial molar heat ($\Delta Q^{\mathrm{int}}/\Delta n_{\mathrm{ads}}$, kJ/mol) as a function of the adsorbed amounts n_{ads} (not reported for the sake of brevity). These values were found virtually identical to the values obtained by differentiating the Q^{int} vs n^{ads} curve (described by a polynomial of order 3 and reported in the inset of section c of the figure, *vide infra*). The cross symbols (present in section a and b only) refer to the adsorption of NH_3 on the same sample but oxidized after exposition to air and subsequently reactivated *in vacuo*. Also in this case, it is clearly evident that the interaction of the probe with the activated sample is not fully reversible under the conditions adopted in the adsorption experiments, in that the 1st and 2nd (obtained after outgassing overnight) runs of adsorption are not coincident. In Table II

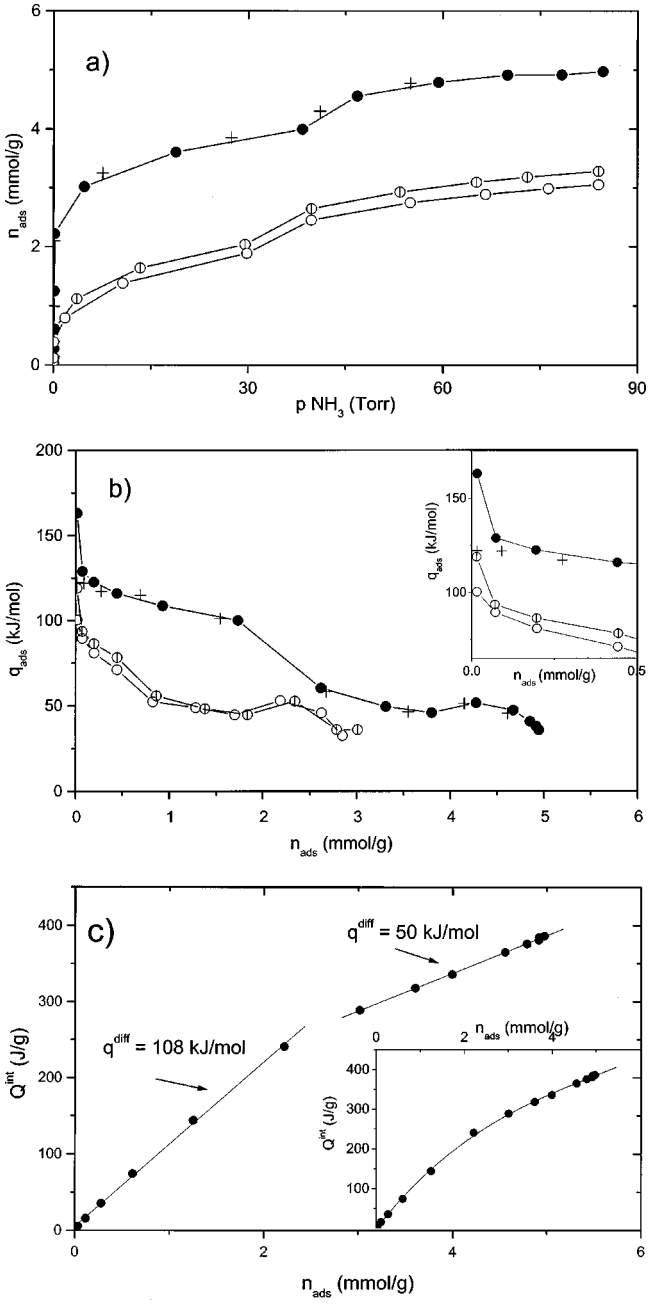

FIG. 7. (a) Volumetric isotherms of NH_3 adsorbed at 303 K on Cu-ZSM-5 activated at 673 K (solid symbol, 1st run; open symbols, 2nd run; barred symbols, 3rd run) and on Cu-ZSM-5 exposed to air and reduced *in vacuo* at 673 K (cross symbols, 1st run). (b) Differential heat of adsorption of NH_3 on the samples described in (a), as a function of the adsorbed amounts. Inset: blow-up of the differential heat of adsorption vs coverage plot at the early stages of the process. Symbols as in (a). (c) Integral heats of adsorption vs adsorbed amounts, fitted separately in the low and high coverage regions. Parameters of linear regression of the low coverage region, $Q^{\mathrm{int}} = a + bn_{\mathrm{ads}}$ ($a = 5.28$; $b = 107.64$; correlation coefficient 0.998 68). Parameters of linear regression of the high coverage region ($a = 139.10$; $b = 49.53$; correlation coefficient of 0.999 19). Inset: integral heats of adsorption vs adsorbed amounts, fitted in the whole coverage interval examined. Parameters of the polynomial regression, $Q^{\mathrm{int}} = a + b_1 n_{\mathrm{ads}} + b_2 n_{\mathrm{ads}}^2 + b_3 n_{\mathrm{ads}}^3$ ($a = -1.60$; $b_1 = 142.34$; $b_2 = 19.28$; $b_3 = 1.26$).

the quantitative and energetic data for the adsorption of NH_3 at $p = 20$ and 80 Torr are reported and compared with those discussed for CO. At an equilibrium pressure of 80 Torr the total adsorbed amounts are much higher than in the case of

CO (4.95 instead of 1.65 mmol/g of zeolite), as expected as a consequence of the strong basic strength of NH_3 with respect to CO. At the same equilibrium pressure the amounts adsorbed during the 2nd run were 3.04 mmol/g of zeolite, corresponding to 61.4% of the total NH_3 adsorbed. The 3rd run isotherm was obtained by outgassing the reversible component for a longer time, 60 h (in the same conditions as for the CO adsorption). In this case the amount adsorbed at $p = 80$ Torr were slightly higher than those adsorbed during the 2nd run, and namely 3.24 mmol/g of zeolite, corresponding to 65.2% of the total amount. Again, in this case too, even a prolonged outgassing at $p \approx 10^{-5}$ Torr is not sufficiently severe to completely destroy the adducts that *cus* Cu(I) cations can form with a base moderately strong, as NH_3 is. The number of NH_3 molecules adsorbed per Cu(I) cation (at a final equilibrium pressure of 80 Torr; see total adsorption, 1st run) was found to be ≈ 4.8. By assuming that all ammonia was adsorbed on copper sites, this datum indicates that tetra-amino complexes such as $[Cu(NH_3)_4]^+$ are formed at each copper site and that an additional amount of ammonia is weakly bound to the zeolite matrix. Among the 4 NH_3 molecules adsorbed at the Cu(I) sites, ≈ 2.5 are lost upon outgassing at $p \approx 10^{-5}$ (see reversible adsorption, 2nd/3rd runs), whereas ≈ 1.5 are irreversibly held at the sites. This means that one half of the cations lose three of the four ligands by outgassing, whereas the other half only two. This datum confirms the presence of two different families of Cu(I) cations, in agreement with what found for CO adsorption (*vide supra* Sec. III C 1). This also agrees with a previous EXAFS study[21] reporting that in Cu-ZSM-5 zeolite two different families of coordinatively unsaturated cations nearly equally populated are present. By comparing the amounts of NH_3 adsorbed on the reactivated sample (cross samples) with the ones adsorbed on the pristine one, no differences were observed, opposite to what was found in the CO case. This is in agreement with the stronger basicity of NH_3 that is less sensitive than CO toward slight differences in Lewis acid strength of coordinatively unsaturated cations.

From an energetic point of view [see Fig. 7(b)], the evolution of the heat of adsorption with coverage is typical of a heterogeneous surface, in that it decreases from an initial very high value down to $\approx 30-40$ kJ/mol. But, opposite to what found in the case of CO, the heat values do not decreased continuously, in that different regions can be distinguished along both 1st run and 2nd/3rd run curves. First, at the very early stages of the adsorption a few defective sites interact quite strongly ($q_0 \approx 180$ kJ/mol) and irreversibly with NH_3. Then a relatively homogeneous family of sites gives rise to a highly energetic ($130 < q_{ads} < 100$ kJ/mol) and irreversible (in the adopted conditions) interaction. A less energetic ($100 < q_{ads} < 50$ kJ/mol) and reversible interaction is also clearly evident in Fig. 7(b). The low energetic and reversible interaction ($q_{ads} \approx 30-40$ kJ/mol) observed at high coverage corresponds to a nonspecific interaction with the zeolite matrix (see Ref. 22). The more energetic values (both irreversible and reversible) are assumed to be specific of the interaction with *cus* Cu(I) cations, able to form amino-complexes of different stability. As for the high q_0 value, it is probably due to the presence of highly defective sites which nature will be revealed by the XPS study (*vide infra*). These sites apparently disappear as a consequence of the oxidation-reduction cycle, in that the initial heat of adsorption on the reactivated sample (cross symbols) is only ≈ 130 kJ/mol, on line with the initial heat values assigned to the specific interaction with Cu(I) cations. In the inset of Fig. 7(b) only the heat values obtained at very low coverage are reported, in order to better put in evidence the differences between the pristine and reactivated sample, as well as the differences between 2nd and 3rd runs curves. The prolonged outgassing indeed allows to destroy an additional quite small fraction of the most energetic amino-complexes, as indicated by the higher initial heat value. However, as indicated by the virtually complete absence of the 130–100 kJ/mol region in the 2nd and 3rd runs curves, the large majority of the more energetic adducts are stable and are not destroyed by outgassing at $p \approx 10^{-5}$ Torr (either only 14 or even 60 h). To better describe the presence of essentially two families of Cu(I) sites capable of binding NH_3, let us consider the integral heats vs coverage curve (1st run of adsorption) reported in Fig. 7(c). In the inset of the figure the Q^{int} vs n_{ads} curve (obtained by a polynomial of order 3; see the parameters in the caption of the figure) is reported. The slope of the curve decreases in the whole range of coverage examined, and two different ranges can be distinguished in the curve. Thus, the low and high coverage regions of the plot were considered separately and a linear fit (see the parameters in the caption of the figure) was satisfactorily obtained for the two different branches of the plot. The differential heat of adsorption for the low coverage branch is 108 kJ/mol and corresponds to a coverage of 2.18 mmol/g zeolite (last point of the low coverage straight line), i.e., to ≈ 2 molecules of NH_3 per Cu(I) cation. The differential heat of adsorption for the high coverage branch is 50 kJ/mol and corresponds to the adsorption of an additional amount of ≈ 2.8 molecules/cation (last point of high coverage straight line: 4.97 mmol/g zeolite, i.e., 4.8 molecules/cation). This datum confirms the formation of the tetra-amino $[Cu(NH_3)_4]^+$ species at the copper sites. The excess of ≈ 0.8 molecules/cation corresponds to the NH_3 physisorbed (via H-bonds) on the residual SiOH groups of the zeolite with a heat of adsorption of 30–40 kJ/mol, as indicated by the values reported in Table II, in agreement with Refs. 22 and 58.

b. IR spectroscopy of adsorbed NH_3: The noncomplete reversibility upon outgassing at RT of the $[Cu(NH_3)_4]^+$ complexes formed at the cationic sites in the zeolite structure was revealed also by IR spectroscopy. In fact, prolonged outgassing at RT up to a final vacuum of 10^{-4} Torr implies a reduction of about 60% of the intensities of the bands ascribed to NH_3: the δ(NH) one at 1610 cm^{-1} and the ν(NH) in the 3500–3100 cm^{-1} interval (not reported for brevity). This quantitative datum is in fair agreement with the reversible amount of ammonia determined by volumetric-calorimetric data (*vide supra*). Finally, no evidence of formation of NH_4^+ cations was detected, confirming once again that we are dealing with a virtually 200% exchanged sample where virtually all H^+ ions have been replaced by Cu^+.

c. XPS spectroscopy of adsorbed NH_3: Opposite to what is observed for CO, where no variation of the C(1*s*)

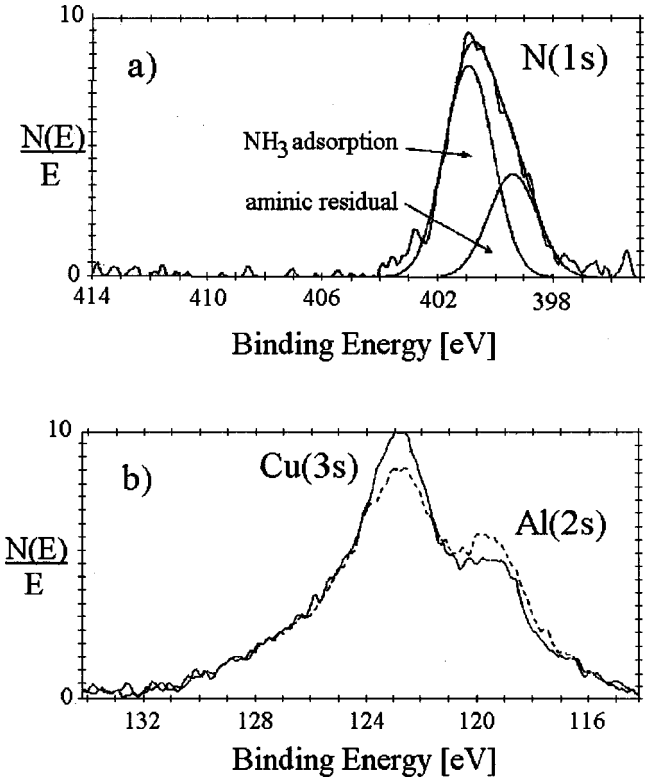

FIG. 8. (a) N(1*s*) XPS peak measured after interaction of NH_3 (10 Torr for 30′) in the prechamber. Its clear asymmetric tail suggest that we are dealing with two different families of nitrogen atoms. Also reported are two Gaussian contributions, and the corresponding sum, resulted after the deconvolution of the experimental curve into two components at 399.4 eV (aminic residual, also present before ammonia dosage) and 400.3 eV (adsorbed NH_3 molecules). (b) XPS spectra in the Cu(3*s*) and Al(2*s*) range before (dotted line) and after (full line) ammonia dosage (10 Torr for 30′).

could be detected, a significant increase of the N(1*s*) signal was observed upon dosing NH_3 on the sample in the prechamber, reflecting an increment of the nitrogen at % from 1.0 (aminic residual from the template burning) to 2.6, see Fig. 8(a). This figure reports the experimental N(1*s*) XPS peak measured after NH_3 dosage, together with its deconvolution into two Gaussian contributions. The deconvolution parameters of the first one were fixed in both position (399.4 eV) and FWHM (2.1 eV) to the values obtained in the spectra measured before ammonia dosage, while those related to the second component were totally free, resulting to be centered at 400.9 eV with a FWHM of 2.0 eV. This experiment definitely proves that a measurable fraction of NH_3 molecules is strongly held on the sample even under severe vacuum conditions as the ones imposed by an XPS experiments.

The surprising datum is that no appreciable variation in position, FWHM and intensity, was observed on the Cu(2*p*), Cu(2*s*) XPS and *LMM* Auger peaks upon interaction with ammonia. On the contrary, the Cu(3*s*) XPS peak seems to undergo a detectable intensity increase, as shown in Fig. 8(b), whereas a simultaneous decrease of the Al(2*s*) peak intensity seems also to occur. The picture emerging from the XPS measurement was for us unexpected and rather puzzling, since (i) we were not able to observe any energy shift in the XPS and Auger peaks of copper, shift expected in the case of formation of $Cu(I)/NH_3$ complexes; (ii) we are so unable to explain where the ammonia molecules, giving rise to the N(1*s*) signal at 400.9 eV, are adsorbed on; (iii) we cannot explain the apparent variation in the surface at % of Cu and Al species emerging from Fig. 8(b) upon ammonia dosage [note also that the increment of the Cu(3*s*) peak intensity is not accompanied by a parallel increase of the other copper features]. We so realized that the reproducibility of these data needed to be checked, and successive NH_3 desorption/adsorption experiments were performed, as summarized in Table III. We see that the behavior of the nitrogen at % is correlated with the adsorption/desorption procedures and is consistent with the hypothesis that a relevant fraction (slightly more than 50%) of NH_3 molecules, are firmly held on the sample at 10^{-9} Torr, even after a thermal treatment *in vacuo* at 723 K. It is worth noticing that in all these experiments no significant modification of the (2*p*), (2*s*) XPS and *LMM* Auger peaks of copper was detected.

In order to explain the XPS results, a totally different attitude must be adopted. We must assume that, as was the case for CO, the Cu(I) sites in ZSM-5 are not able to retain ammonia molecules at 10^{-9} Torr. This will explain the constant behavior of the (2*p*), (2*s*) XPS and *LMM* Auger peaks of copper. To be consistent with this hypothesis, we must of course assume that also the Cu(3*s*) peak remains unaffected by ammonia dosage and we must find an alternative model for the adsorption of ammonia, in order to explain the results of Fig. 8(a).

On the basis of the chemical affinity of NH_3, its interaction with a zeolite matrix can involve different kinds of highly energetic adsorbing sites. (i) Due to its basic character, a preferential interaction will occur with Lewis acid sites. Now, the most common Lewis acid sites in zeolites are the counterions [Cu(I), in our case] but a small fraction of very strong Lewis acid sites can be formed when one or more Al–O–Si bridges are broken resulting in trigonal Al(III) *cus* species. (ii) Ammonia can interact with residual H^+ Brønsted sites resulting in the formation of ammonium species. (iii) It can dissociate on a strained T–O–T bridge resulting in $T–NH_2\cdots HO–T$ groups. It is worth noticing that the total amount of each kind of defective sites are, in the volume of the sample, below the detection threshold of IR spectroscopy.

TABLE III. Nitrogen at % from the evaluation of N(1*s*) XPS signal in successive NH_3 desorption/adsorption experiments. In desorption experiments the sample is heated in the prechamber up to 723 K for 2 h.

Sample treatment	Virgin	$+NH_3$ 10 Torr for 30′	Outgassed at 723 K for 2 h	$+NH_3$ 10 Torr for 40′	Outgassed at 723 K for 2 h
Nitrogen at %	1.0	2.6	1.8	2.7	2.0

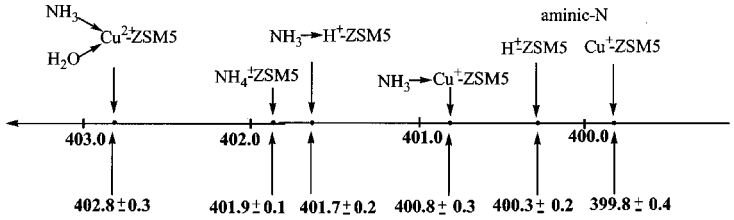

FIG. 9. Calibration scale for N(1*s*) XPS peak for different amino-complexes in different zeolitic environments.

It is evident that all points (i)–(iii) would contribute to the N(1*s*) peak, while only point (i), when the Lewis site is a trigonal Al(III) species or point (iii), if one of the two T atoms is an aluminum, would affect the Al(2*s*) peak. It is evident that in all cases we are dealing with highly reactive phenomena, where ammonia molecules are supposed to be adsorbed very strongly, to be irreversibly held even at 10^{-9} Torr and, in some cases, to be partially held after a thermal treatment up to 723 K. It is worth noticing that the formation of species (i)–(iii) is also able to explain the presence of a small fraction of very energetic sites giving rise to heat of adsorption values as high as 180 kJ/mol, *vide supra* Fig. 7. In fact, comparable values were observed upon ammonia adsorption on both acidic zeolites[59] and high surface area aluminas.[60]

Coming to the quantitative aspect of this phenomena, we see from Fig. 7 that about 1% of the total NH_3 molecules adsorbed at 80 Torr are those involved in the formation of the high-energy complexes. To evaluate the order of magnitude of the phenomenon on a quantitative ground, let us suppose that all NH_3 molecules, giving rise to the 180 kJ/mol value, are adsorbed on defective Al(III) sites. Now, since at 80 Torr we have observed the formation of $[Cu(NH_3)_4]^+$ complexes we can affirm that the defective Al(III) species represents at most 4% of the extra framework Cu(I) species, and thus of the regular $[Al(OSi)_4]$ species. A fraction of defective Al(III) species as low as 4% is certainly not able to explain the modification of the XPS spectra reported in Fig. 8(b) from which a fraction of 20% is inferred. Once again, this discrepancy is only apparent, since the 4% value obtained by volumetric-calorimetric data reflects the fraction measured on all sites of both internal and external surfaces, while in the value estimated from XPS, the external surface sites are largely preponderant. We can so conclude that defective Al(III) species are much more abundant at the external surface of our Cu(I)-ZMS-5 sample rather than in the internal one. This conclusion really makes sense, since the external surface of the zeolite crystals can be considered as defects of an ideally infinite crystal, where at least one Al–O–Si bond has been broken.[61,62]

D. Determination of a calibration scale for N(1*s*) XPS peaks in a zeolitic environment

As already discussed in Sec. III A, a carbon–nitrogen contamination was present as a consequence of the template (tetra-propyl-ammonium) burning. In this case, the N(1*s*) peak, recorded on the Cu-ZSM-5 surface, had a symmetrical shape centered at 399.8±0.4 eV. For the sake of comparison the H-ZSM-5 zeolite, obtained after thermal decomposition of the ammonium counterion [see Eq. (1), but without gas phase exchange with CuCl], was also considered and the aminic residual (already inside) appeared as a N(1*s*) peak shifted towards higher BE (400.3±0.2 eV). This difference could be considered negligible. However, the same two samples (Cu-ZSM-5 and H-ZSM-5) were analyzed after NH_3 adsorption (10 Torr, RT), when N(1*s*) peak reached about 3 at % of relative concentration. The so obtained N(1*s*) peaks were not symmetrical because their maxima were shifted towards higher BE (401.7±0.2 eV for H-ZSM-5; 400.8±0.3 eV for Cu-ZSM-5), and previous N contamination remained and appeared as shoulders at lower BE. The energy separation of the two N(1*s*) peaks, after NH_3 adsorption, was around 1 eV. These values are no longer similar, suggesting the possibility of different interaction sites for them. So that, whether NH_3 on Cu-ZSM-5 resulted from XPS analysis in a strong interaction with defective Al(III) species (*vide supra*), on H-ZSM-5 ammonia prefers to interact with protons yielding to the formation of ammonium after the following gas/solid reaction,

$$Si–(OH)^+–Al^- + NH_3 \rightarrow Si–(ONH_4)^+–Al^-, \quad (4)$$

which is the inverse path of reaction (1), strongly favored at RT. By considering the two cases for aminic-nitrogen and the other two for ammonic-nitrogen, taken with the same zeolite, it can be observed that the energy separation for Cu-ZSM-5 and H-ZSM-5 are comprised between 1.0 eV and 1.4 eV. This value represents the chemical shift due to the transition from aminic to ammonic nitrogen and is schematically reported in Fig. 9.

Another comparison was carried out directly on the original NH_4-ZSM-5 zeolite, synthesized using the ammonium as counterion. In that case, the N(1*s*) peak appeared at 401.9±0.1 eV, to be compared with the peak at 401.7±0.2 eV obtained upon dosing NH_3 on the H-ZSM-5 zeolite (*vide supra*). Due to the broadness of these XPS peaks we must conclude that the ammonium ions in ZSM-5 are virtually identical whatever included during the synthesis or obtained after reaction (4).

The highest value of BE was observed by considering the interaction of NH_3 with a Cu(II)-ZSM-5, obtained by exposing Cu(I)-ZSM-5 to the atmosphere (see Sec. III B). The corresponding BE value resulted 402.8±0.3 eV. The BE scale reported in Fig. 9 reflects nitrogen species that more and more increase their oxidation state, by partially losing their electronic charge, donated to progressively more electrofilic ligands. This comparison regarding different BE of the electronic level N(1*s*) is allowed only because the nitro-

gen environment is almost the same as in all cases, assuring that the long range potentials do not change significantly as far as the same zeolitic matrix is considered. Otherwise different Madelung potentials would play an important role.

IV. CONCLUSIONS

The Cu(I)⇔Cu(II) redox chemistry in a Cu-ZSM-5 was investigated by means of XPS and XANES spectroscopies. It has been found that all copper sites are virtually able to perform the complete Cu(I)→Cu(II)→Cu(I) redox cycle. This implies that all Cu sites are potentially active sites in the de-NO_x reactions. CO and NH_3 were used as probe molecules in order to assess the coordinative unsaturation of the Cu(I) cations. The quantitative and energetic aspects of the formation of carbonyl-like and amino-complexes at the metallic sites were studied by means of adsorption microcalorimetry while the spectroscopic aspects were investigated by IR and XANES. The formation at RT under a pressure of gas of 80 Torr of $[Cu(CO)_2]^+$ and $[Cu(NH_3)_4]^+$ complexes has been reported. A significant fraction of CO and NH_3 molecules are irreversibly held on Cu(I) sites even after outgassing at RT in a final dynamical vacuum of 10^{-5} Torr. XPS spectroscopy indicates that $[Cu(CO)_n]^+$ and $[Cu(NH_3)_m]^+$ complexes are totally destroyed at 10^{-9} Torr. This experimental evidence implies a serious reconsideration of what was generally considered as a ''stable adduct.'' A significant amount of NH_3 was found to be irreversibly held on defective sites as revealed by both XPS and calorimetry. The amounts estimated by XPS results were much higher than those estimated by volumetric-calorimetric data, indicating that the defects present in the system are mainly concentrated at the external surface of zeolite crystals. Finally, from the complete set of XPS measurements a calibration scale for the N(1*s*) peak in various nitrogen species in different zeolite samples is proposed.

ACKNOWLEDGMENTS

We thank P. Fisicaro, E. Giamello, and A. Zecchina for fruitful discussions. X-ray absorption measurements have been performed at the BM8 GILDA beamline at the ESRF within the public user program (Ref. 25). The authors are also indebted to all the GILDA technical staff (in particular to F. Danca) and to ESRF Chem. Lab. (in particular to Dr. Müller), who have allowed us to work under optimal conditions. The GILDA beamline is financed by INFM, INFN, and CNR. The present work is part of a project coordinated by A. Zecchina and cofinanced by the Italian MURST (Cofin 98, Area 03). One of us (Gemma Turnes Palomino) is thankful to the European Community for a TMR grant.

[1] W. M. Meier, D. H. Olson, and Ch. Baerlocher, *Atlas of Zeolite Structure Types* (Elsevier, London, 1996).
[2] R. M. Szostak, *Molecular Sieves* (Van Nostrand Reinhold, New York, 1989).
[3] J. M. Thomas, R. G. Bell, and C. R. A. Catlow, in *Handbook of Heterogeneous Catalysis*, edited by G. Ertl, H. Knözinger, and J. Weitkamp (VCH, Weinheim, 1997), pp. 286–310.
[4] W. J. Mortier, *Compilation of Extra Framework Sites in Zeolites* (Butterworth, London, 1981).
[5] A. Zecchina and C. Otero Areán, Catal. Rev. Sci. Eng. **35**, 261 (1993).
[6] Y. Iwasawa, in *Handbook of Heterogeneous Catalysis*, edited by G. Ertl, H. Knönzinger, and J. Weitkamp (VCH, Weinheim, 1997), pp. 853–873.
[7] H.-F. Freund, Angew. Chem. Int. Ed. Engl. **36**, 453 (1997).
[8] A. Zecchina, D. Scarano, S. Bordiga, G. Spoto, and C. Lamberti, Adv. Catal. (in press), and references therein.
[9] M. Iwamoto, H. Furukawa, Y. Mine, F. Umera, S. Mikuriya, and S. Kagawa, Chem. Soc. Chem. Commun. **1986**, 1272.
[10] M. Iwamoto and H. Hamada, Catal. Today **10**, 57 (1991).
[11] M. Shelef, Chem. Rev. **95**, 209 (1995), and references therein.
[12] ZSM-5 is a silicon-rich zeolite with MFI structure (Refs. 1–3) showing a three-dimensional pore system consisting of two intersecting sets of tubular channels (~5.5 Å in diameter) defined by 10-member rings of TO_4 tetrahedra.
[13] K. C. C. Kharas, D.-J. Liu, and H. J. Robota, Catal. Today **26**, 129 (1995).
[14] Y. Kuroda, Y. Yoshikawa, S. Konno, H. Hamano, H. Maeda, R. Kumashiro, and M. Nagao, J. Phys. Chem. **99**, 10621 (1995).
[15] S. Tanabe and H. Matsumoto, Bull. Chem. Soc. Jpn. **63**, 192 (1990).
[16] M. Iwamoto, H. Yahiro, K. Tanada, N. Mizumo, Y. Mine, and S. Kagawa, J. Phys. Chem. **95**, 3727 (1991).
[17] W. Grünert, N. W. Hayes, R. W. Joyner, E. S. Shpiro, M. Rafiq, H. Siddiqui, and G. N. Baeva, J. Phys. Chem. **98**, 10832 (1994).
[18] H. Hamada, N. Matsubayashi, H. Shimada, Y. Kintaichi, T. Ito, and A. Nishijima, Catal. Lett. **5**, 189 (1990).
[19] G. Spoto, S. Bordiga, D. Scarano, and A. Zecchina, Catal. Lett. **13**, 39 (1992).
[20] G. Spoto, A. Zecchina, S. Bordiga, G. Ricchiari, G. Martra, G. Leofanti, and G. Petrini, Appl. Catal., B **3**, 151 (1994).
[21] C. Lamberti, S. Bordiga, M. Salvalaggio, G. Spoto, A. Zecchina, F. Geobaldo, G. Vlaic, and M. Bellatreccia, J. Phys. Chem. B **101**, 344 (1997), and references therein.
[22] V. Bolis, S. Bordiga, C. Lamberti, A. Zecchina, G. Petrini, F. Rivetti, and G. Spanò, Langmuir **15**, 5753 (1999); Microporous Mesoporous Mater. **30**, 67 (1999).
[23] V. Bolis, C. Morterra, M. Volante, L. Orio, and B. Fubini, Langmuir **6**, 695 (1990).
[24] S. Pascarelli, F. Boscherini, F. D'Acapito, C. Meneghini, J. Hrdy, and S. Mobilio, J. Synchrotron Radiat. **3**, 147 (1996).
[25] S. Bordiga, A. Zecchina, G. Lamberti, M. Salvalaggio, G. Spoto, and F. D'Acapito, ESRF Proposal CH-542, BM8 GILDA beamline, 10-14/10/1998.
[26] J. F. Moulder, W. F. Stickle, P. E. Sobol, and K. D. Bomben, *Handbook of X-Ray Photoelectron Spectroscopy*, edited by J. Chastain (Perkin–Elmer, Eden Prairie, 1992).
[27] B. A. Sexton, T. D. Smith, and J. V. Sanders, J. Electron Spectrosc. Relat. Phenom. **35**, 27 (1985).
[28] I. Jirika and V. Bosachek, Zeolites **11**, 77 (1991).
[29] E. S. Shpiro, W. Grünert, R. W. Joyner, and G. N. Baeva, Catal. Lett. **24**, 159 (1994).
[30] C. Dossi, A. Fusi, G. Moretti, S. Recchia, and R. Psaro, Appl. Catal., A **188**, 107 (1999).
[31] C. Dossi, S. Recchia, A. Pozzi, A. Fusi, V. Dalsanto, and G. Moretti, Phys. Chem. Chem. Phys. **1**, 4515 (1999).
[32] I. C. Hwang and S. I. Woo, J. Phys. Chem. B **101**, 4055 (1997).
[33] S. Contarini and L. Kevan, J. Phys. Chem. **90**, 1630 (1986).
[34] G. J. Millar, A. Canning, G. Rose, B. Wood, L. Trewartha, and I. D. R. Mackinnon, J. Catal. **183**, 169 (1999).
[35] C. Lamberti, G. Spoto, D. Scarano, C. Pazé, M. Salvalaggio, S. Bordiga, A. Zecchina, G. Turnes Palomino, and F. D'Acapito, Chem. Phys. Lett. **269**, 500 (1997).
[36] C. Lamberti, S. Bordiga, A. Zecchina, M. Salvalaggio, F. Geobaldo, and C. Otero Areán, J. Chem. Soc., Faraday Trans. **94**, 1519 (1998).
[37] G. Turnes Palomino, P. Fisicaro, E. Giamello, S. Bordiga, C. Lamberti, and A. Zecchina, J. Phys. Chem. B **104**, 4064 (2000).
[38] Y. Kuroda, H. Maeda, Y. Yoshikawa, R. Kumashiro, and M. Nagao, J. Phys. Chem. B **101**, 1312 (1997).
[39] R. Kumashiro, Y. Kuroda, and M. Nagao, J. Phys. Chem. B **103**, 89 (1999).
[40] D.-J. Liu and H. J. Robota, J. Phys. Chem. B **103**, 2755 (1999).
[41] C. Lamberti, G. Turnes Palomino, S. Bordiga, G. Berlier, F. D'Acapito, and A. Zecchina, Angew. Chem. Int. Ed. Engl. **39**, 2138 (2000).
[42] A. W. Aylor, S. C. Larsen, J. A. Reimer, and A. T. Bell, J. Catal. **157**, 592 (1995).
[43] Y. Li and W. K. Hall, J. Catal. **129**, 202 (1991).
[44] J. Sàrkàny, J. L. d'Itri, and W. M. H. Sachtler, Catal. Lett. **16**, 241 (1992).

[45] W. K. Hall and J. Vaylon, Catal. Lett. **15**, 311 (1992).
[46] J. Valyon and W. K. Hall, J. Phys. Chem. **97**, 7054 (1993).
[47] H. J. Jong, W. K. Hall, and J. L. d'Itri, J. Phys. Chem. **100**, 9416 (1996).
[48] T. Cheung, S. K. Bhargava, M. Mobday, and K. Foger, J. Catal. **158**, 301 (1996).
[49] It is worth recalling that the features of the XANES spectra (i.e., position and intensity of the peaks in both pre- and near-edge regions) depend on both oxidation and coordination states of the adsorbing atom. This explains the differences observed in the XANES spectra of model compound with well defined oxidation state, e.g., Cu_2O vs CuCl or CuO vs $CuCl_2$. This means that an accurate XANES study must be done on the basis of a complex multiple scattering approach [see, e.g., T. A. Tyson, K. O. Hodgson, C. R. Natoli, and M. Benfatto, Phys. Rev. B **46**, 5997 (1992), and references therein]. Unfortunately this kind of study can be done only for well defined systems, where the geometry around the absorbing atom can be clearly defined, as was the case of $[Cu(CO)_3]^+$ complexes in the C_{3v} configuration observed in Cu(I)-ZSM-5 at 80 K (Ref. 41). Here, we are dealing with a rather inhomogeneous family of copper sites (as clearly pointed out in Secs. III C 3 a and III C 3 b by our microcalorimetric study) and thus the determination of a well defined cluster defining the local environment of copper, needed for an accurate modeling of the XANES spectra, cannot be done. Notwithstanding this limitation, Solomon and co-workers (Ref. 50) after a systematic XANES study of 19 Cu(I) and 40 Cu(II) model compounds, proposed the ''normalized difference edge'' method for a quantitative determination of Cu(I) content in copper complexes of mixed oxidation state composition. Note that the reason why this method gives so good results lies in the fact that no Cu(II) complex exhibit significant feature below 8985 eV.
[50] L.-S. Kau, D. J. Spira-Solomon, J. E. Penner-Kahn, K. O. Hdgson, and E. I. Solomon, J. Am. Chem. Soc. **109**, 6433 (1987), and references therein.
[51] N. J. Blackburn, R. W. Strange, J. Reedijk, A. Volbeda, A. Farooa, K. D. Karin, and J. Zubieta, Inorg. Chem. **28**, 1349 (1989), and references therein.
[52] A. Zecchina, S. Bordiga, M. Salvalaggio, G. Spoto, D. Scarano, and C. Lamberti, J. Catal. **173**, 540 (1998).
[53] G. Spoto, S. Bordiga, G. Ricchiardi, D. Scarano, A. Zecchina, and F. Geobaldo, J. Chem. Soc., Faraday Trans. **91**, 3285 (1995).
[54] V. Bolis, S. Bordiga, V. Graneris, C. Lamberti, G. Turnes Palomino, and A. Zecchina, Stud. Surf. Sci. Catal. **130**, 3261 (2000).
[55] A. Zecchina, S. Bordiga, G. Turnes Palomino, D. Scarano, C. Lamberti, and M. Salvalaggio, J. Phys. Chem. B **103**, 3833 (1999).
[56] D. Scarano, P. Galletto, C. Lamberti, R. De Franceschi, and A. Zecchina, Surf. Sci. **387**, 236 (1997).
[57] V. Bolis, G. Magnacca, and C. Morterra, Res. Chem. Intermed. **25**, 25 (1999); C. Lamberti, S. Bordiga, F. Geobaldo, A. Zecchina, and C. Otero Areán, J. Chem. Phys. **103**, 3158 (1995); V. Bolis, S. Bordiga, C. Lamberti, G. Turnes Palomino, and A. Zecchina (unpublished).
[58] S. Bordiga, I. Roggiero, P. Ugliengo, A. Zecchina, V. Bolis, G. Artioli, R. Buzzoni, G. L. Marra, F. Rivetti, G. Spanó, and C. Lamberti, J. Chem. Soc., Dalton Trans. (in press).
[59] A. Auroux, V. Bolis, P. Wierzchowski, P. C. Gravelle, and J. C. Védrine, J. Chem. Soc., Faraday Trans. 2 **75**, 2544 (1979).
[60] A. Auroux and A. Gervasini, J. Phys. Chem. **94**, 6371 (1990).
[61] M. Trombetta and G. Busca, J. Catal. **187**, 521 (1999).
[62] M. Trombetta, T. Armaroli, A. Gutierrez Alejandre, J. Ramirez, and G. Busca, Appl. Catal., A **192**, 125 (2000).